ELSEVIER

Biochimica et Biophysica Acta 1466 (2000) 245–259

BIOCHIMICA ET BIOPHYSICA ACTA
BBA

www.elsevier.com/locate/bba

A Fourier transform infrared spectroscopic study of the interaction of alkaline earth cations with the negatively charged phospholipid 1,2-dimyristoyl-*sn*-glycero-3-phosphoglycerol

Patrick Garidel, Alfred Blume, Wigand Hübner *

Martin-Luther-University Halle-Wittenberg, Institute of Physical Chemistry, Muehlpforte 1, D-06108 Halle/Saale, Germany

Received 21 September 1999; received in revised form 9 February 2000; accepted 11 February 2000

Abstract

The interaction of aqueous phospholipid dispersions of negatively charged 1,2-dimyristoyl-*sn*-glycero-3-phosphoglycerol, sodium salt (DMPG) with the divalent cations Mg^{2+}, Ca^{2+} and Sr^{2+} at equimolar ratios in 100 mM NaCl at pH 7 was investigated by Fourier transform infrared spectroscopy. The binding of the three cations induces a crystalline-like gel phase with highly ordered and rigid all-*trans* acyl chains. These features are observed after storage below room temperature for 24 h. When the gel phase is heated after prolonged incubation at low temperature phase transitions into the liquid crystalline phase are observed at 58°C for the DMPG:Sr^{2+}, 65°C for the DMPG:Mg^{2+}, and 80°C for the DMPG:Ca^{2+} complex. By subsequent cooling from temperatures above T_m these complexes retain the features of a liquid crystalline phase with disordered acyl chains until a metastable gel phase is formed at temperatures between 38 and 32°C. This phase is characterized by predominantly all-*trans* acyl chains, arranged in a loosely packed hexagonal or distorted hexagonal subcell lattice. Reheating the DMPG:Sr^{2+} samples after a storage time of 2 h at 4°C results in the transition of the metastable gel to the liquid crystalline phase at 35°C. This phase transition into the liquid crystalline state at 35°C is also observed for the Mg^{2+} complex. However, for DMPG:Mg^{2+} at higher temperatures, a partial recrystallization of the acyl chains occurs and the high temperature phase transition at 65°C is also detected. In contrast, DMPG:Ca^{2+} exhibits only the phase transition at 80°C from the crystalline gel into the fluid state upon reheating. Below 20°C, the rate of conversion from the metastable gel to a thermodynamically stable, crystalline-like gel phase decreases in the order $Ca^{2+} \gg Mg^{2+} > Sr^{2+}$. This conversion into the crystalline gel phase is accompanied by a complete dehydration of the phosphate groups in DMPG:Mg^{2+} and by a reorientation of the polar lipid head groups in DMPG:Ca^{2+} and in DMPG:Sr^{2+}. The primary binding sites of the cations are the PO_2^- groups of the phosphodiester moiety. Our infrared spectroscopic results suggest a deep penetration of the divalent cations into the polar head group region of DMPG bilayers, whereby the ester carbonyl groups, located in the interfacial region of the bilayers, are indirectly affected by strong hydrogen bonding of immobilized water molecules. In the liquid crystalline phase, the interaction of all three cations with DMPG is weak, but still observable in the infrared spectra of the DMPG:Ca^{2+} complex by a slight ordering effect induced in the acyl chains, when compared to pure DMPG liposomes.

Keywords: Phosphatidylglycerol; Ion binding; Divalent cation; Fourier transform infrared spectroscopy; Lipid–cation interaction

* Corresponding author. Fax: +49-345-55-27157; E-mail: huebner@chemie.uni-halle.de

0005-2736/00/$ – see front matter
PII: S0005-2736(00)00166-8

1. Introduction

The study of the interaction of divalent cations with liposomes is of great interest, because a number of biological processes, such as membrane fusion, enzyme regulation and signal transduction, are induced by the association of cations with negatively charged lipids of natural membranes [1–8]. As an example, Fragata et al. [9] have shown that a specific association of phosphatidylglycerol and Mg^{2+} ions leads to a structural and functional optimization of the photosystem II complex.

In the past, experiments with different physical techniques have been performed to understand the interaction of di- and multivalent cations with negatively charged phospholipids in bilayer membranes [10–27]. A two step binding model was proposed [28], in which the first step describes the diffuse electrostatic attraction of the metal ions to the negatively charged bilayer surface. In the following second step the cation penetrates the head group water interface and forms a complex with one or more lipid phosphate groups. This kind of interaction to individual phosphate sites has been postulated in phosphatidic acid:calcium complexes by Papahadjopoulos et al. [29] and Laroche et al. [30].

In a recent study, we have investigated the binding of alkaline earth cations Mg^{2+}, Ca^{2+} and Sr^{2+} to the anionic phospholipid 1,2-dimyristoyl-*sn*-glycero-3-phosphoglycerol (DMPG) by differential scanning (DSC) and isothermal titration calorimetry (ITC) as a function of temperature, lipid:cation molar ratio and thermal history of the samples [31]. Our DSC results indicated, depending on the metal ion, different stable and metastable DMPG:divalent cation complexes. From the higher phase transition temperatures and enthalpies of DMPG:Ca^{2+}, compared to the Sr^{2+} and Mg^{2+} analogues, it was concluded that calcium forms the most stable complexes with DMPG and also a different gel phase structure was suggested. Moreover, our ITC experiments can be interpreted as hydrophobic dehydration in the presence of divalent cations. In accordance with a larger binding enthalpy, this effect is much more pronounced for Ca^{2+} than for Mg^{2+} or Sr^{2+}.

Fourier transform infrared spectroscopy (FTIR) has been proven to be well suited to detect changes in the structure of hydrocarbon chains [32–35] by monitoring the frequencies of the acyl chain vibrational modes with respect to external parameters such as temperature [36–38], cation concentration [39–41] or thermal history of the samples [42,43]. In addition, variations in hydration, hydrogen bonding, and/or polarity at specific sites of the bilayer molecules can be localized [44–47].

In this FTIR spectroscopic study we use the advantages of the technique to differentiate between the hydrophobic part and the interfacial region of DMPG bilayers with the aim of localizing the binding places of the divalent cations calcium, magnesium, and strontium and elucidating the structural changes within the hydrophobic and hydrophilic part of the bilayers induced by the binding process.

2. Materials and methods

2.1. Materials

DMPG was purchased from Lipoid KG (Ludwigshafen, Germany) and Enzymatix Ltd. (Cambridge, UK). The purity of the lipids was checked by thin layer chromatography (TLC). After detection with a phosphorus sensitive spray and charring with concentrated sulfuric acid [48], only one spot was detected on the TLC plate. Therefore, the lipids were used without further purification.

Calcium chloride dihydrate, magnesium chloride hexahydrate, strontium chloride hexahydrate and sodium chloride of analytical grade were obtained from E. Merck, Darmstadt (Germany).

2.2. Sample preparation

Multilamellar DMPG lipid dispersions were prepared by adding 100–150 μl of a solution of 100 mM NaCl in H_2O or in D_2O to $\sim$10 mg of dry lipid. The samples were heated to temperatures above the gel to liquid crystalline phase transition temperature of the phospholipid ($T > T_m$+10°C), sonicated at low power with a Bandelin sonotrode (Sonoplus, HD 60, Berlin, Germany), equipped with a 4.5 mm titanium tip, for 15–30 s and then incubated at temperatures above the phase transition of the lipid for an additional 45 min. The pH of the samples was checked and adjusted to the desired value.

1:1 molar ratio complexes of lipid to alkaline earth cation were prepared by adding the appropriate amount of salt (1 M salt solution in water at pH 7) to obtain an equimolar mixture of DMPG and salt. The samples were again sonicated as described above and incubated at 80°C for 45 min.

2.3. Instrumentation

Lipid dispersions (~50 μl) were placed in 50 or 25 μm thick infrared cells with demountable BaF_2 windows. The hollow window mounts were thermostated by an external thermostat. Temperature control was achieved by a digital thermometer interfaced to a computer using a PT 100 resistor fixed close to the cell windows. Spectra were recorded with a Bruker IFS 48 and IFS 66 v/s Fourier transform infrared spectrometer equipped with an MCT detector. 512 interferograms were collected, apodized with a triangular function and Fourier transformed after one level of zero filling. The spectral resolution of the FTIR spectra was 2 cm^{-1} with encoding data points every 1 cm^{-1}.

2.4. Data analysis

Spectra of 100 mM NaCl in H_2O (or D_2O) were used as references and subtracted from those spectra of aqueous lipid dispersions that were recorded at equal temperatures (±0.1 K). The baseline in the carbonyl and phosphate region was not completely flat. Therefore, a linear baseline with constant slope was subtracted in the spectral region of interest. Peak positions were determined by applying second derivative spectroscopy and using the center of gravity algorithm, supplied by the Bruker software. The spectra of the phosphate, the CH_2 stretching, and the CH_2 scissoring modes were obtained from FTIR measurements of lipids in H_2O, those of the carbonyl mode from measurements of lipid dispersions in D_2O.

3. Results

3.1. The hydrophobic core

3.1.1. CH_2 stretching vibrations

The CH_2 stretching vibrations give rise to bands in the spectral region from 3100 to 2800 cm^{-1}, with the CH_2 antisymmetric and symmetric stretching modes located at ~2920 and ~2850 cm^{-1}, respectively. The frequencies of these bands are conformation sensitive and respond to temperature induced changes of the *trans–gauche* ratio of carbon–carbon bonds in the acyl chains. An increased proportion of *gauche* conformers in the acyl chains corresponds to a shift of the absorption maxima of both CH_2 stretching vibrations to higher frequencies [36].

Fig. 1 shows the frequency of the maximum of the symmetric CH_2 stretching bands $\nu_s(CH_2)$ of DMPG and DMPG:divalent cation complexes (1:1 molar ratio) at pH 7 as a function of temperature after incubation of the samples at 4°C for 24 h. The phase transition from the gel to the liquid crystalline phase is marked by an abrupt change in the frequencies of the $\nu_s(CH_2)$ mode. For the pure lipid DMPG in 100 mM NaCl (in the absence of divalent cations), this phase transition is observed at ~24°C. The addition of divalent cations shifts the phase transition to higher temperatures. Upon heating the samples, the beginning of the chain melting process of DMPG:Sr^{2+}, DMPG:Mg^{2+} and DMPG:Ca^{2+}, located at 58°C, 65°C and 80°C respectively, is marked by a large increase in frequency ($\Delta\nu_s \approx 4$ cm^{-1}). From Fig. 1 we also infer that the binding of the divalent cations to the lipid bilayer leads to an increase in conformational order of the hydrocarbon chains. This is reflected in the absolute values of the symmetric CH_2 stretching bands at temperatures below the phase transition (closed symbols in Fig. 1). Compared to free, uncomplexed DMPG, the frequencies of the $\nu_s(CH_2)$ band of the divalent cation complexes are shifted by 1 cm^{-1} from 2850 cm^{-1} to lower values. The low frequency of the $\nu_s(CH_2)$ band at 2849 cm^{-1} in the gel phase of all DMPG:divalent cation complexes is an indication for a tight packing of immobilized all-*trans* acyl chains.

Above their respective phase transitions, the $\nu_s(CH_2)$ frequencies for DMPG, DMPG:Sr^{2+} and DMPG:Mg^{2+} are identical and the increase to more than 2853 cm^{-1} with temperature is characteristic for phospholipids with acyl chains in the liquid crystalline state. The frequency values of 2852 cm^{-1} for DMPG:Ca^{2+} at temperatures above 85°C differ from those of the strontium and magnesium complexes at the same temperature. These results can

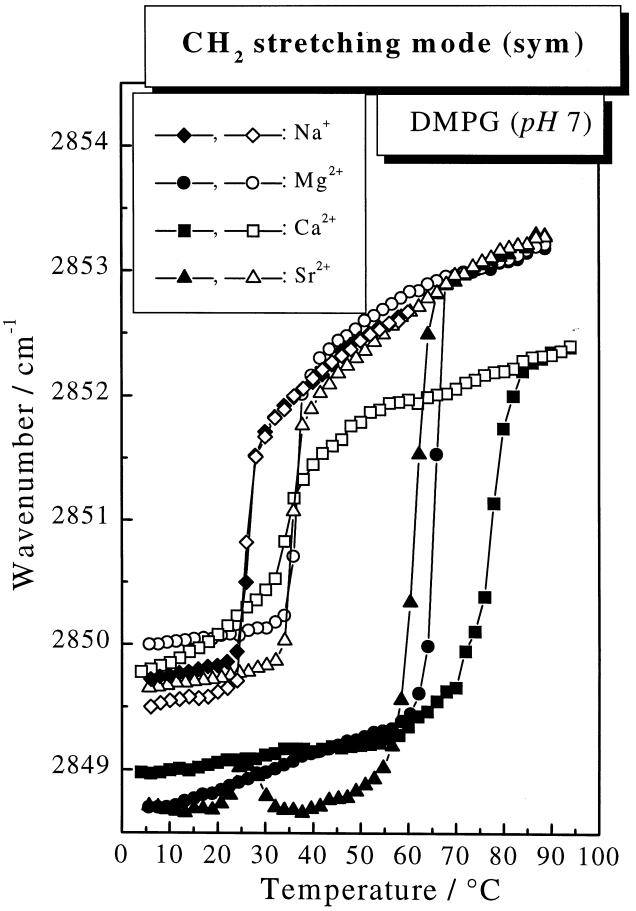

Fig. 1. Temperature dependence of the symmetric CH_2 stretching mode frequency of DMPG:Na^+ (diamonds) and of the equimolar complexes DMPG:Mg^{2+} (circles), DMPG:Ca^{2+} (squares) and DMPG:Sr^{2+} (triangles) in 100 mM NaCl at pH 7. Solid symbols represent the heating and open symbols the cooling scan. The samples were stored for 24 h at 4°C prior to the first cycle.

be explained by fewer *gauche* conformers in the liquid crystalline phase, probably induced by a weak but distinct interaction of calcium ions with the lipid head groups in the fluid state.

Besides the usually observed linear increase in frequency with temperature within the gel and liquid crystalline phases of the samples, the frequency vs. temperature plot for the DMPG:Sr^{2+} complex indicates a small maximum at 24°C. The abrupt increase of the $\nu_s(CH_2)$ band is due to the melting of a small fraction of uncomplexed DMPG, but the immediately following drop in frequency is the consequence of an isothermal recrystallization process, induced by the binding of strontium ions to lipid molecules in the fluid state.

Fig. 1 also shows subsequently following cooling scans of the Ca^{2+}, Mg^{2+} and Sr^{2+} complexes and of the Na^+ salt of DMPG (open symbols, Fig. 1). In contrast to the pure DMPG liposome system that converts to the gel state at the expected temperature of 24°C upon cooling (see rhombic symbols in Fig. 1) the phase transition of the three DMPG:divalent cation complexes exhibits a large hysteresis upon cooling. The $\nu_s(CH_2)$ band frequency decreases only slightly upon cooling from 90 to 35°C but at 35°C a sharp drop is observed. Furthermore, we notice a discrepancy between the frequencies of the $\nu_s(CH_2)$ stretching modes at the beginning of the first heating and the end of the first cooling scans (see low temperatures in Fig. 1). The $\nu_s(CH_2)$ band positions of the cooling scans at 10°C are 1 cm^{-1} higher when compared to the corresponding temperature of the heating scan and comparable to those of pure DMPG in the gel state. This indicates differences in the conformation of the acyl chains of the DMPG:divalent cation complexes before and after the first heating and cooling cycle. From our observations we conclude that metastable phases, e.g. an undercooled liquid crystalline phase and a metastable gel phase, are formed upon cooling.

During the cooling cycle when the temperature is already below 35°C the recrystallization process proceeds faster for the DMPG:Ca^{2+} than for the other two complexes. This can be inferred from the larger slope of the frequency vs. temperature plot between 35 and 10°C. An incubation time of 2–5 h at low temperature after the cooling scan leads to a conformational ordering of the acyl chains of the DMPG:Ca^{2+} complexes, indicated by a significant decrease of the $\nu_s(CH_2)$ frequencies to values from the beginning of the first heating scan. In contrast to DMPG:Ca^{2+}, the thermodynamically stable gel phases of DMPG:Mg^{2+} and DMPG:Sr^{2+} are obtained only after an annealing process below 20°C for at least 24 h. Therefore, the thermotropic phase behavior of these systems is extremely sensitive to the history of the sample preparation.

Fig. 2 indicates the second heating and cooling cycle of the samples after an incubation time of 2 h at 4°C. As mentioned above, the frequencies of the $\nu_s(CH_2)$ stretching vibration of DMPG:Ca^{2+} are lo-

cated around 2849 cm^{-1} at low temperatures and the phase transition is again observed at 80°C. However, the change of the slope in the frequency vs. temperature plot between 45–65°C reveals minor conformational ordering effects of hydrocarbon chains in the crystalline state.

During the second heating run of DMPG:Mg^{2+}, two phase transitions are clearly visible. The metastable gel phase formed during the first cooling scan melts at 35°C, but immediately above this temperature recrystallization takes place by rebinding of released magnesium ions, probably induced and accelerated by nucleation lipids present in the crystalline state. However, the observed frequency decrease up to 55°C does not indicate a complete recrystallization of the system. At 65°C the proportion of crystalline DMPG:Mg^{2+} formed between 40 and 55°C and during the incubation time of 2 h at 4°C exhibits the transition to the liquid crystalline state.

For DMPG:Sr^{2+}, the incubation time of 2 h at 4°C is too short to convert the metastable gel phase at least partially to the crystalline phase. Therefore, the frequency of the $\nu_s(CH_2)$ stretching vibration of 2849.7 cm^{-1} at the beginning of the second heating cycle in Fig. 2 matches the frequency at the end of the first (and second) cooling cycle in Fig. 1 and only one phase transition at 35°C is observed upon reheating the sample.

The cooling scans of the second cycle of all samples (see open symbols in Fig. 2) exhibit the sharp frequency drop between 35 and 40°C, characteristic for the transition of a metastable liquid crystalline to the metastable gel phase.

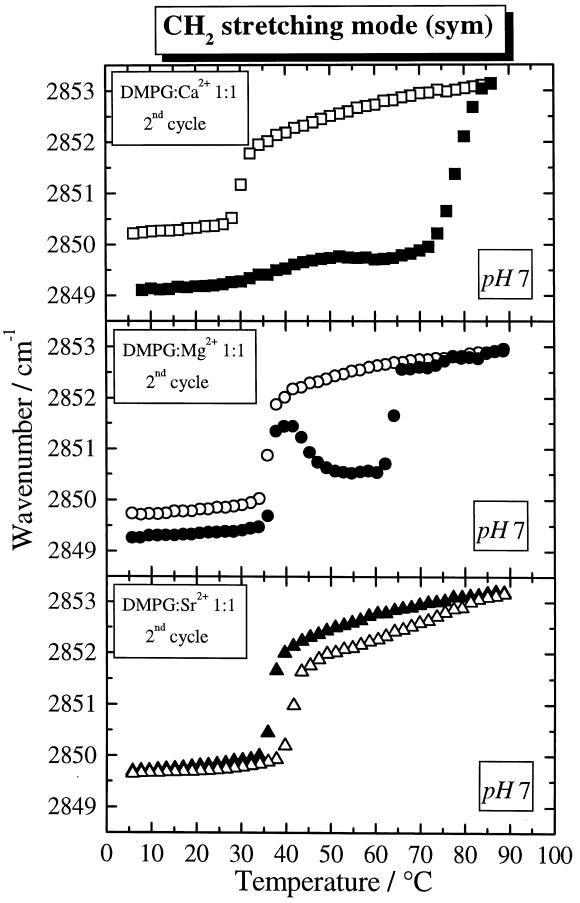

Fig. 2. Temperature dependence of the symmetric CH_2 stretching mode frequency of the equimolar complexes DMPG:Ca^{2+} (squares), DMPG:Mg^{2+} (circles), and DMPG:Sr^{2+} (triangles) in 100 mM NaCl at pH 7 (second cycle). The IR spectra were registered 2 h after the first heating and cooling cycle. Solid symbols represent the heating and open symbols the cooling scan.

3.1.2. CH_2 scissoring vibrations

The frequencies of the scissoring vibrations of the methylene and methyl groups are located in the 1500–1350 cm^{-1} region. The CH_2 scissoring mode gives rise to bands around 1470 cm^{-1}; the number and frequencies of these bands are dependent on the acyl chain packing and conformation [32,33,36,49]. Parallel aligned all-*trans* hydrocarbon chains packed in a triclinic subcell lattice reveal a CH_2 scissoring band maximum at 1473 cm^{-1}, whereas a band maximum at 1468 cm^{-1} is indicative for a hexagonal packing of all-*trans* methylene chains and/or orientational disorder of the hydrocarbon chains. A splitting of this band into two components at 1462 cm^{-1} and 1472 cm^{-1} appears by interchain vibrational coupling in an orthorhombic subcell lattice with the planes of ordered all-*trans* acyl chains being arranged perpendicular to each other. The antisymmetric and umbrella-type symmetric deformation modes of the methyl groups occur as additional bands with low intensity in this spectral region around 1460 cm^{-1} and 1380 cm^{-1} respectively [33].

In Fig. 3 are shown the scissoring bands of uncomplexed and divalent cation complexed DMPG. The dotted lines in Fig. 3 display the corresponding inverted second derivatives of the methylene scissoring bands. In this figure spectra at 6°C before the

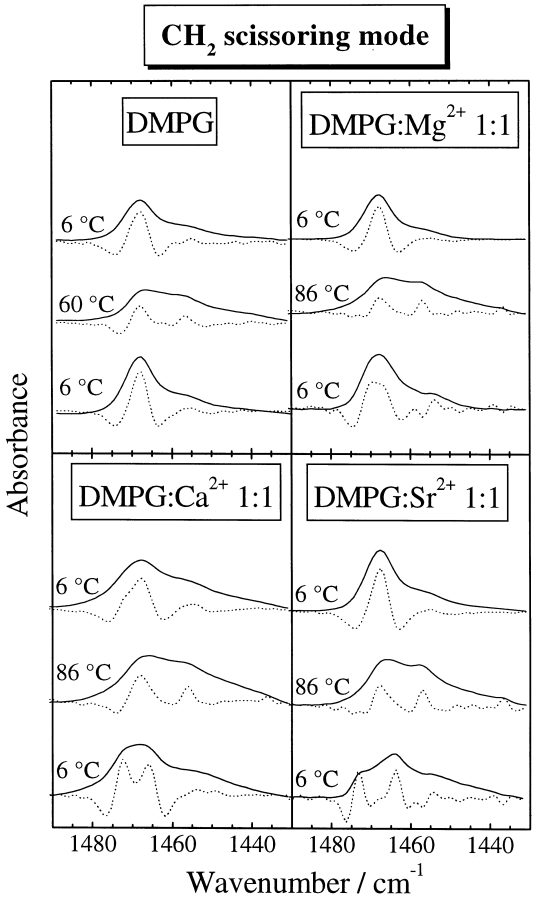

Fig. 3. CH_2 scissoring mode (solid line) of DMPG (Na^+ salt) and of the equimolar complexes DMPG:Mg^{2+}, DMPG:Ca^{2+} and DMPG:Sr^{2+} in 100 mM NaCl at pH 7. The bottom spectrum in each panel shows the corresponding band after storage of the samples at 4°C for 24 h, the middle spectrum the band of the samples in the liquid crystalline phase and the top spectrum the corresponding band immediately after the first cooling cycle. Inverted second derivative spectra are represented by dotted lines.

first heating scan, obtained after an incubation time of 24 h (bottom spectra of Fig. 3), at a temperature above the phase transition (middle spectra of Fig. 3), and after the end of the succeeding cooling scan at low temperature (top spectra of Fig. 3) are compared.

The uncomplexed DMPG reveals a scissoring band maximum around 1468 cm^{-1} at all temperatures, indicative for hydrocarbon chains arranged in a hexagonal subcell lattice without interchain interactions. Below T_m, the all-*trans* acyl chains undergo rapid rotational and/or torsional motions around their long axis. Above the gel to liquid crystalline phase transition temperature T_m, the increased mobility and the higher portion of *gauche* conformers of the methylene groups in the acyl chains lead to a broadening and an intensity decrease of the scissoring band at 1467 cm^{-1} [36]. Snyder proposed assigning the band around 1458 cm^{-1} to the scissoring mode of methylene groups adjoining a *trans* bond and a *gauche* bond [33]. Following this interpretation the increased intensity between 1455 and 1460 cm^{-1} relative to the area at 1467 cm^{-1} in DMPG and in the DMPG:divalent cation complexes above T_m is representative for the introduction of *gauche* conformers.

Cooling the samples of the DMPG:divalent cation complexes to temperatures below 35°C leads to a reduction in bandwidth of the 1468 cm^{-1} absorption and to a drastic decrease in band intensity at 1458 cm^{-1}. The spectra of DMPG:Mg^{2+} and DMPG:Sr^{2+}, obtained at the end of the first (or second) cooling cycle at 6°C, are comparable to the spectrum of DMPG at 6°C (see top spectra in Fig. 3). These features with the narrower CH_2 scissoring band at 1468 cm^{-1} reveal the typical gel phase spectra of phospholipids with all-*trans* acyl chains loosely packed in a hexagonal subcell lattice, in which reorientational motions around the long axis of the molecules are not completely damped out. In contrast the DMPG:Ca^{2+} spectrum, obtained under the same conditions of cooling at 6°C, exhibits an increased halfwidth of the band around 1467 cm^{-1} and the resolution enhanced spectrum reveals a high frequency shoulder at 1472 cm^{-1}. This is a consequence of increased interchain interaction induced by the beginning of chain recrystallization and can be interpreted by a gradual change from a hexagonal over a distorted hexagonal towards an orthorhombic subcell lattice and by a concomitant decrease in reorientational motions.

After an incubation time of 24 h at low temperature (see spectra at 6°C at the bottom of Fig. 3) this recrystallization process is advanced and the two components of the CH_2 scissoring band at 1464 and 1473 cm^{-1} are clearly visible in the second derivative spectra of DMPG:Ca^{2+} and DMPG:Sr^{2+}. For DMPG:Mg^{2+} the recrystallization process after 24 h of annealing at 6°C is only signified by a broadening of the scissoring band at 1468 cm^{-1} and by a flat topped second derivative spectrum. One explan-

ation for the badly resolved two component bands in DMPG:Mg^{2+} might be an angle different from 90° between neighboring planes of all-*trans* acyl chains normally found in orthorhombic subcells, or frozen-in twisted methylene chains diminishing the vibrational coupling between neighboring molecules.

3.2. The interfacial region

3.2.1. The carbonyl bands

The most useful infrared bands for probing the phospholipid interfacial region are the ester C=O double bond vibrations of the two acyl chains. These $\nu_{C=O}$ absorption bands are sensitive to changes in the polarity of their local environments and are influenced by hydrogen bonding and other interactions with appropriate ligands [46]. Changes in the contours of the $\nu_{C=O}$ absorption bands can often be interpreted in terms of structural and/or hydration changes of the bilayer polar/apolar interface [43,44,46]. In general, in hydrated samples only a broad band contour is found for the ester C=O stretching vibrations in the 1750–1700 cm^{-1} region. However, resolution enhancement techniques usually reveal two or more underlying component bands.

Fig. 4 displays the carbonyl stretching region of the pure phospholipid DMPG at pH 7 and of the corresponding complexes at low temperature in the crystalline state (bottom spectra in Fig. 4), above the phase transition in the liquid crystalline state (middle) and immediately after the cooling cycle in the metastable gel state (top spectra in Fig. 4).

In the gel phase, the overall C=O band maximum of DMPG occurs between 1740 and 1737 cm^{-1} and in the liquid crystalline phase between 1733 and 1731 cm^{-1}. The broad band contour is the summation of at least two subcomponent bands with maxima near 1742 and 1727 cm^{-1}. The relative intensities of these component bands reflect the contribution of subpopulations of free and hydrogen bonded carbonyl groups [44,50]. In the liquid crystalline phase of DMPG, the increased intensity of the underlying component band at 1727 cm^{-1}, attributed to a higher amount of hydrogen bonded carbonyl groups, broadens the band and shifts its maximum to lower frequencies. The carbonyl band contours of the DMPG:divalent cation complexes in the liquid crystalline phase exhibit the same shape as pure DMPG.

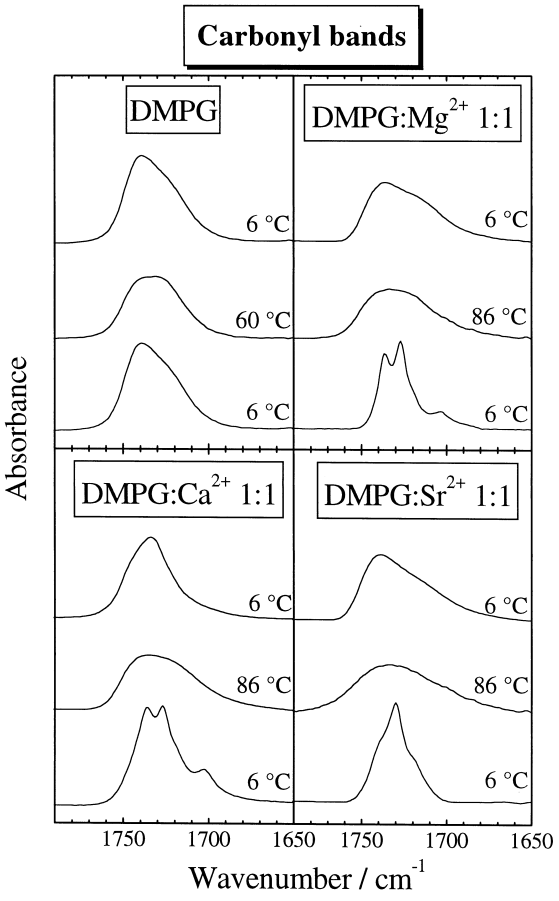

Fig. 4. Carbonyl bands of DMPG (Na^+ salt) and of the equimolar complexes DMPG:Mg^{2+}, DMPG:Ca^{2+} and DMPG:Sr^{2+} in 100 mM NaCl in D_2O at pH 7. The bottom spectrum in each panel shows the corresponding bands after storage of the samples at 4°C for 24 h, the middle spectrum the band of the samples in the liquid crystalline phase and the top spectrum the corresponding band immediately after the first cooling cycle.

Upon cooling to 6°C, the metastable gel phase of DMPG:Mg^{2+} and DMPG:Sr^{2+} reveals carbonyl band shapes similar to those found for DMPG in the gel phase indicating decreased intensity of the component band at 1727 cm^{-1}. The carbonyl vibrational band of the DMPG:Ca^{2+} complex, obtained after cooling the sample from 90°C to 6°C differs in shape, its frequency maximum being shifted to 1730 cm^{-1}. Again, the onset of the recrystallization process in DMPG:Ca^{2+} is responsible for these differences.

Low temperature incubation at 4°C for 24 h dramatically changes the contours of the carbonyl bands of the DMPG:divalent cation complexes (see bottom

spectra in Fig. 4). In these crystalline phases, the fine structure of the spectra is attributed to immobilized carbonyl groups located in different environments. In the complexes of DMPG:Ca^{2+} and DMPG:Mg^{2+}, three narrow bands at 1737 cm^{-1}, 1727 cm^{-1} and 1702 cm^{-1} are clearly resolved and can be assigned to non-hydrogen bonded and hydrogen bonded carbonyl groups. Carbonyl vibrations with extremely low frequencies between 1710 and 1702 cm^{-1} have also been found in crystalline calcium and magnesium phosphatidylserine complexes [39–41,51,52] and can only be explained by very strong hydrogen bonding of trapped and immobilized water molecules. In the crystalline DMPG:Sr^{2+} complex, the low frequency carbonyl band at 1702 cm^{-1} is absent but instead a third less structured hydrogen bonded carbonyl band at 1717 cm^{-1} has emerged. From this observation we conclude that in the crystalline phase of DMPG:Sr^{2+} the water molecules in the interfacial region are less immobilized.

3.2.2. The phosphate bands

Another hydration sensitive group of infrared bands arising from phospholipid head group vibrations originates from the phosphodiester moiety. Two strong bands in the range 1260–1215 cm^{-1} and 1110–1080 cm^{-1} arise from the antisymmetric and symmetric PO_2^- stretching vibrations, while the single bond P–O stretching modes are observed at lower frequencies (900–800 cm^{-1}). The frequency of the antisymmetric stretching vibration $\nu_{as}(PO_2^-)$ in fully hydrated phospholipid samples with phosphodiester moieties is found at about 1220–1225 cm^{-1}. In dry samples, this band is shifted to about 1250 cm^{-1}. The symmetric PO_2^- absorption band $\nu_s(PO_2^-)$ of dry lipid samples is only shifted by about 5 cm^{-1} to higher values [47].

In Fig. 5, the spectral region between 1350 and 950 cm^{-1} for the Na^+ salt of DMPG above and below the phase transition of $T_m = 24°C$ is displayed. Although this spectral region is crowded by the presence of several overlapping bands, the features observed at 1230–1210 cm^{-1} ($\nu_{as}(PO_2^-)$) and at 1100–1080 cm^{-1} ($\nu_s(PO_2^-)$) can unambiguously be assigned to the PO_2^- antisymmetric and symmetric stretching modes, respectively.

Unfortunately, the infrared spectra of hydrocarbon chains in all-*trans* conformation display a series of sharp and equispaced bands in the region 1350–1190 cm^{-1}, the methylene wagging band progressions. In the gel phase of lipids, especially at low temperature, these bands are superimposed onto the PO_2^- antisymmetric stretching component [36,53] and demonstrate that the acyl chains are mainly in the ordered all-*trans* conformation. For phospholipids with ordered dimyristoyl acyl chains, the first band is always found at about 1204 cm^{-1} and the last band at 1325 cm^{-1}. The number of these bands is $n/2$ with $n = 12$ for the number of CH_2 units within the myristoyl chain [53]. The six progression bands in the gel phase spectrum of DMPG at pH 7 are separated by 20–26 cm^{-1} and assigned in Fig. 5. We have used the best resolved progression band at 1280 cm^{-1} as the marker band for the appearance of all-*trans* acyl chains in all investigated DMPG:divalent cation systems.

Due to a higher proportion of *gauche* conformers and/or to *gauche*/*trans*/*gauche* conformers (gtg) next to the carbonyl end of the *sn*-1 acyl chain these progression bands decrease in intensity with increasing temperature and disappear completely at T_m.

At T_m, no changes in the frequency of the symmetric and antisymmetric PO_2^- vibrations at 1090 and 1217 cm^{-1} are observed. Therefore, the frequency and bandshape of both phosphate bands are not or only weakly dependent on the phase state of DMPG. However, the frequency at 1217 cm^{-1} for the $\nu_{as}(PO_2^-)$ band maximum of the hydrated DMPG is 5–8 cm^{-1} lower than for comparable phospholipids like DMPC (1,2-dimyristoyl-*sn*-glycero-3-phosphocholine), where the $\nu_{as}(PO_2^-)$ band is found at $\sim$1225 cm^{-1}. In lipids which have the ability to form a hydrogen bonding network, like phosphatidylethanolamines or DMPG, we observe this band at $\sim$1217 cm^{-1} (see top spectrum in Fig. 5). Such a low frequency for $\nu_{as}(PO_2^-)$ has also been described by Goni and Arrondo for cardiolipin [54]. In these lipids strong hydrogen bonds with the phosphate group are expected and can be realized either by direct interaction of OH glycerol groups of DMPG and cardiolipin with the phosphate groups or by interaction with intercalated and immobilized water molecules.

In addition to the symmetric and antisymmetric PO_2^- stretching bands at 1090 cm^{-1} and at 1217 cm^{-1} and the wagging band progression in the spectrum of DMPG, a strong band at 1068 cm^{-1} with a

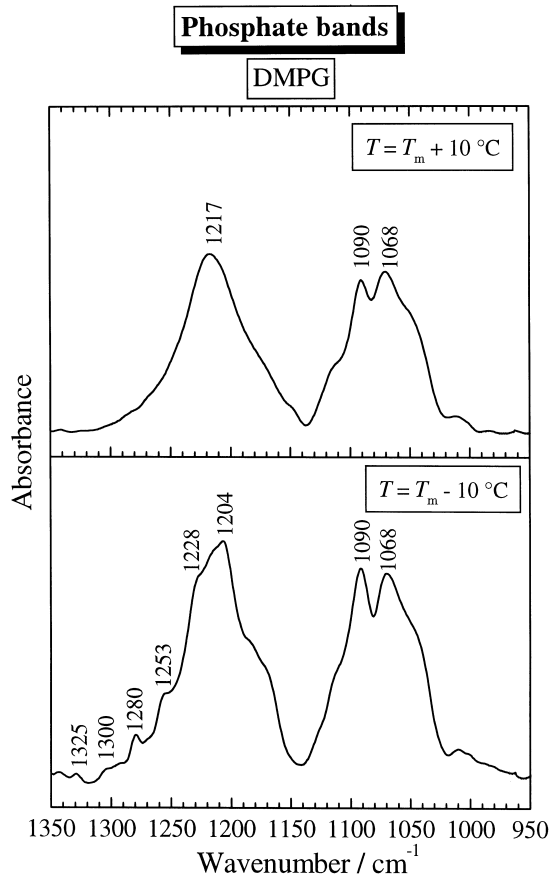

Fig. 5. Spectral region of the PO_2^- stretching bands of DMPG in 100 mM NaCl at pH 7 below (bottom) and above (top) the gel to liquid crystalline phase transition temperature (T_m = 24°C). The indicated frequencies between 1200 and 1350 cm^{-1} in the bottom spectrum are assigned to the methylene wagging band progression of all-*trans* acyl chains.

shoulder at 1050 cm^{-1} is observed, which is always found in phosphodiester compounds. Following the assignment of Arrondo and Goni [54] this absorption is due to the two C–O–P stretching modes of the phosphodiester moiety $\nu(C^{glycerol}–O–(P))$ and $\nu(C^{head}–O–(P))$. This signal is therefore attributed to the R–O–P–O–R′ head group vibration.

The two shoulders around 1170 cm^{-1} and 1120 cm^{-1} (Fig. 5) originate from vibrations of the CO–O single bond vibrations of the carbonyl ester groups and from C–O stretching modes, most probably from the glycerol C–O–H groups.

In Figs. 6–8 the spectral region of 1350–950 cm^{-1} is shown as a function of temperature for the equimolar complexes of DMPG:Ca^{2+}, DMPG:Mg^{2+} and DMPG:Sr^{2+}, as obtained from the first and second heating and cooling cycles. At the bottom of Figs. 6–8 are plotted the corresponding spectra of the heating scan starting from low temperature and from the middle to the top the succeeding spectra of the cooling scan to low temperature are displayed.

In the spectrum of the DMPG:Ca^{2+} complex, the methylene progression bands overlapping the $\nu_{as}(PO_2^-)$ band decrease in intensity and disappear above 80°C in the heating scan. In the following cooling scan they reappear below 38°C (see arrows at 1280 cm^{-1} in Fig. 6). This is in accordance with the two phase transitions from the crystalline to the liquid crystalline and from the metastable liquid crystalline to the metastable gel state, also revealed as a shift of the symmetric CH_2 stretching vibration at 80°C upon heating and at around 35°C upon cooling (see Figs. 1 and 2). The transition from the crystalline to the liquid crystalline phase can also be monitored in the head group by a broadening of the antisymmetric PO_2^- stretching vibration band above 76°C.

In contrast to the spectra of the region of the symmetric PO_2^- stretching vibration between 1120 and 950 cm^{-1} obtained for the liquid crystalline and the metastable gel phase of DMPG:Ca^{2+}, which resemble the spectra of DMPG in Fig. 5, the spectra for crystalline DMPG:Ca^{2+}, obtained after incubation at 4°C for 24 h, are completely different (see left panel in Fig. 6). The broad bands at 1090 cm^{-1} and 1068 cm^{-1} have changed to at least six sharp and characteristic bands at 1122, 1105, 1080, 1060, 1035 and 985 cm^{-1}. A similar spectral pattern has been reported for crystalline ox brain calcium phosphatidylserine (PS) complexes [51] and was rationalized in terms of a formation of a bidentate PS–Ca^{2+} complex. The higher number of vibrational bands was explained by a lower symmetry at the PO_2^- site upon binding of calcium to the negatively charged oxygens of the phosphate moiety, thus resulting in the splitting of degenerated modes by the introduction of previously inactive infrared vibrations. In addition, this band splitting pattern in the $\nu_s(PO_2^-)$ region of dry and hydrated calcium complexes of saturated and unsaturated phosphatidylserine bilayers has been interpreted by Casal et al. [41,55] with a change of two torsion angles of the two P–O ester bonds in R–O–P–O–R′ from *gauche–gauche*, usually found in phosphate esters to antiplanar–anti-

planar. From these results we infer that the binding of calcium to the PO_2^- groups of DMPG induces a crystalline phase with a rearrangement of the R–O–P–O–R′ head group moiety to an antiplanar–antiplanar conformation.

We have mentioned before that reheating and cooling the samples 2 h after the first cycle has a different impact on the organization of the lipid acyl chains in the Ca^{2+}, Mg^{2+} and Sr^{2+} complexes (see Fig. 2). In the right panel of Fig. 6 this behavior is shown for the spectral region 1350–950 cm^{-1} of the Ca^{2+} complex and can be explained by changes in the interfacial region. A comparison with the spectra of the second cycle of the other two complexes (right panels in Figs. 7 and 8) reveal that the band of the antisymmetric PO_2^- stretching vibration of the Ca^{2+} complex at low temperature between 1260 and 1180 cm^{-1} is superimposed by intensive absorptions of the progression bands. The appearance of the wagging band progressions and their band intensities reveals a kinetically driven behavior, because after the incubation time of only a few hours at low temperature (~4°C) a reorganization of the hydrocarbon chains of DMPG:Ca^{2+} is induced.

With increasing temperature, the intensity of the wagging band progressions becomes smaller due to a small increase of *trans–gauche* isomerizations. This leads to the appearance of a narrow antisymmetric phosphate band at 1225 cm^{-1} just below 50°C. Above 50°C the antisymmetric and symmetric phosphate band shapes are dramatically changed with increasing temperature (see spectra at 56°C in Fig. 6, right panel). The $\nu_{as}(PO_2^-)$ band centered at ~1225 cm^{-1} splits into two band components above 50°C. With increasing temperature only the low frequency component at 1215 cm^{-1}, revealing a different hydrogen bonding pattern, is observed. At 86°C this band becomes broader and is slightly shifted to 1217 cm^{-1}.

The spectral region between 1150 and 950 cm^{-1} of the calcium complex also exhibits very complicated features. Below 50°C this spectral region is marked by three bands: two sharp ones at ~1112 and ~1010 cm^{-1} and a broad one with a maximum centered at 1065 cm^{-1}. No band at 985 cm^{-1} is detected. Between 50 and 80°C the characteristic pattern of the crystalline phase of DMPG:Ca^{2+} with the six bands at 1122, 1105, 1080, 1060, 1035 and 985 cm^{-1} has

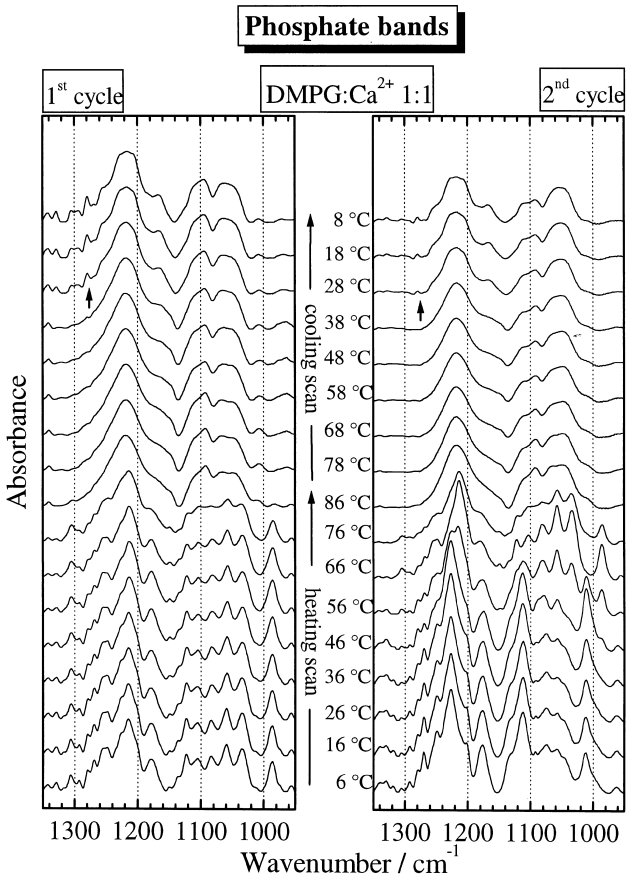

Fig. 6. Spectra of the phosphate spectral region for the first and second heating and cooling cycles of the equimolar complex DMPG:Ca^{2+} in 100 mM NaCl at pH 7 (start: bottom of the figure). Arrows indicate the appearance of the wagging band progression in the cooling scans.

emerged. Our interpretation for these phenomena in the DMPG:Ca^{2+} spectra of the second heating cycle between 45 and 60°C is a reorientation and recrystallization of the polar head groups and a transformation from a metastable crystalline state to the stable crystalline state, whereby the acyl chains are only slightly affected (see also Fig. 2).

For the metastable crystalline phase (bottom spectra in Fig. 6, right panel), the spectra of the head group region seem not to be a mixture of those of the stable crystalline phase (bottom spectra in Fig. 6, left panel) and of the metastable gel phase obtained directly after the first cooling cycle (top spectra in Fig. 6, left panel), because the sharp band at 1010 cm^{-1} is not detected in these phases and moreover the band at 985 cm^{-1}, typical for the stable crystal-

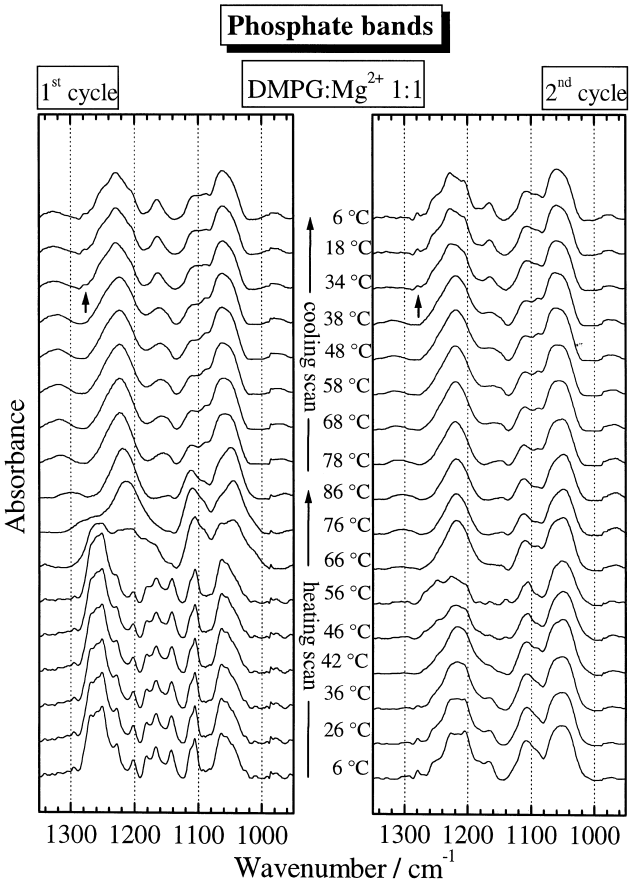

Fig. 7. Spectra of the phosphate spectral region for the first and second heating and cooling cycles of the equimolar complex DMPG:Mg^{2+} in 100 mM NaCl at pH 7 (start: bottom of the figure). Arrows indicate the appearance of the wagging band progression in the cooling scans.

line phase, is completely absent in the metastable crystalline phase.

The stable crystalline phase of DMPG:Mg^{2+} exhibits a different behavior in the interfacial region. The antisymmetric PO_2^- stretching band maxima at 1260 cm^{-1} in the bottom spectra of the left panel of Fig. 7, though overlapped by the wagging progression bands, unambiguously indicate completely dehydrated phosphate groups. However, the binding of Mg^{2+} ions does not induce a reorientation of the polar head groups, because the symmetric PO_2^- stretching band is only shifted from 1095 to 1102 cm^{-1}, which can be explained by the dehydration effect, but the complex band splitting pattern of crystalline DMPG:Ca^{2+} is not observed. The narrow bands of the $\nu_s(PO_2^-)$ vibrations and of the R–O–P–O–R′ moiety at 1060 cm^{-1} indicate immobilized head groups.

The phase transition of DMPG:Mg^{2+} from the crystalline to the liquid crystalline state is indicated in the spectrum at 66°C of the first heating cycle by the disappearance of the progression bands, by a broadening of all bands and by a shift of the $\nu_{as}(PO_2^-)$ vibration from 1260 cm^{-1} to lower frequencies. Above this temperature, the band position at 1217 cm^{-1} reveals hydrated phosphate head groups. The appearance of the metastable gel state with hydrated head groups in the following cooling cycle is again indicated in the spectrum at 34°C by an arrow, which marks the progression band at 1280 cm^{-1}.

The second heating cycle of DMPG:Mg^{2+} represents the melting of the metastable gel phase between 36 and 42°C (see bottom spectra of the right panel in Fig. 7). However, between 46 and 60°C a partial recrystallization of the fluid phase to the crystalline gel phase with a partial dehydration and immobilization of the phosphate groups occurs. The spectrum at 56°C of the second heating scan exhibits increased intensity of the antisymmetric PO_2^- vibration at 1260 cm^{-1}, progression bands of low intensity and a structured symmetric PO_2^- band at 1102 cm^{-1}, and can be assigned to a mixture of the crystalline and the liquid crystalline states. Above the phase transition temperature of 65°C the phosphate groups are again completely hydrated and the metastable gel phase reappears after cooling in the spectrum at 34°C.

The spectra of the crystalline phase of DMPG:Sr^{2+} obtained after an incubation time of 24 h at 4°C are shown at the bottom of the left panel of Fig. 8. Below 24°C the phosphate group is hydrated but the region of the symmetric PO_2^- stretching vibration does not exhibit the pattern of crystalline DMPG:Ca^{2+}. As derived from the CH_2 stretching vibrations of Fig. 2 a small amount of unbound DMPG molecules melts at 24°C and above this temperature a recrystallization takes place. This is also reflected in Fig. 8 in the spectra between 1150 and 950 cm^{-1} of the first heating scan of DMPG:Sr^{2+}. Between 36 and 56°C the binding of the strontium ions to the phosphate moiety indicates the same conformation of the immobilized head groups as in the stable crystalline phase of DMPG:Ca^{2+}. By cooling from temperatures above

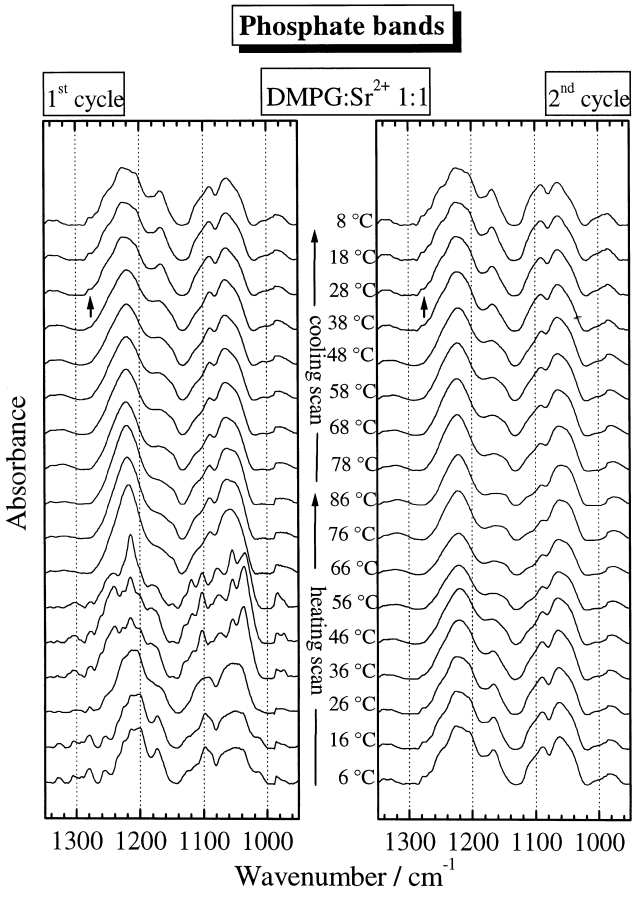

Fig. 8. Spectra of the phosphate spectral region for the first and second heating and cooling cycles of the equimolar complex DMPG:Sr^{2+} in 100 mM NaCl at pH 7 (start: bottom of the figure). Arrows indicate the appearance of the wagging band progression in the cooling scans.

the phase transition of 58°C the spectra of the metastable gel phase are obtained below 38°C. In the second and following heating and cooling cycles only the conversion from the metastable gel to the liquid crystalline state and vice versa are obtained at temperatures between 35 and 40°C (see right panel of Fig. 8).

In the liquid crystalline phase minor differences in the spectral region of the symmetric PO_2^- stretching vibration between DMPG, DMPG:Ca^{2+}, DMPG:Mg^{2+} and DMPG:Sr^{2+} indicate weak binding effects of the divalent cations to the phosphate moieties of the lipids (compare spectra at high temperatures in Figs. 5–8). However, at the moment we cannot interpret these small differences at a molecular level.

4. Discussion

The binding of alkaline earth cations to negatively charged phospholipids leads to gross changes in the thermotropic behavior. The binding of these cations induces a tighter packing of the acyl chains compared to pure DMPG. This process occurs most rapidly in the presence of calcium ions. The tight packing of the hydrocarbon chains in the gel phase implies that the number of *trans–gauche* isomers is reduced. This was proved in our infrared spectra by the appearance of strong wagging band progressions and a low frequency of the symmetric CH_2 stretching band vibration. In the stable/metastable liquid crystalline phase of these systems the interaction of the divalent cations with the DMPG bilayers is strongly reduced but a small increase in conformational order of the fluid hydrocarbon chains is observed for DMPG:Ca^{2+}.

A Raman study of the interaction of the alkaline earth cations Mg^{2+}, Ca^{2+}, and Ba^{2+} with phosphatidylglycerol (DPPG, 1,2-dipalmitoyl-*sn*-glycero-3-phosphoglycerol) performed by Susi [56] confirmed this behavior. These Raman data showed that calcium ions at a molar concentration as low as DPPG:Ca^{2+} 1:0.1 did increase the number of *trans* C–C bonds and the lateral order of DPPG liposomes both below and above the gel to liquid crystalline phase transition temperature. The transition temperature remains essentially unchanged at this calcium cation concentration. Higher concentrations of Ca^{2+} cations wipe out the transition in the studied temperature region of 0–60°C, and result in a markedly higher number of *trans* bonds, as well as a higher lateral order. A comparison between the effects of Mg^{2+}, Ca^{2+}, and Ba^{2+} ions at a molar concentration of 3:1 showed that the calcium ions exhibit by far the strongest effect on the hydrocarbon chain packing of DPPG liposomes. Ba^{2+} ions increase the phase transition temperature; Mg^{2+} ions wipe it out within the studied temperature range. Susi concluded that the effects of these cations on DPPG go beyond simple interaction with the charged head groups of the phospholipids. Reference is made in this connection to the charge induced tilt of the long, aliphatic chains, which has been established also for DPPG [16]. Charge compensation, which is one effect of divalent cations among others, leads to a vanishing

of the tilt and the results obtained by Raman spectroscopy may be correlated with this mechanism [56]. These arguments are in agreement with our experimental results.

The different packing behavior of the DMPG acyl chains in the presence of divalent cations compared to the uncomplexed lipid can also be seen by analyzing the CH_2 scissoring mode. The divalent cations induce a reorganization of the hydrocarbon chains of DMPG from a loosely packed hexagonal towards a distorted hexagonal or orthorhombic subcell lattice. Longer incubation times at low temperature for the Ca^{2+} and Sr^{2+} complex induce stronger interchain interactions and reorientational/torsional motions along the acyl chain axes are damped out.

The influence of the divalent cations in the interfacial region of DMPG was probed by our investigations of the ester carbonyl vibrations. Although for all stable crystalline DMPG:divalent cation complexes an X-ray spectroscopic investigation [57] revealed a small lamellar repeat distance between 4.45 and 4.75 nm (20°C), which must be interpreted as a loss of interbilayer water, the carbonyl groups are still hydrated. Our FTIR spectra indicate a mixture of immobilized hydrated and non-hydrated carbonyl groups. Additional immobilized water molecules are present in the interfacial region of crystalline DMPG:Ca^{2+} and DMPG:Mg^{2+}, as revealed by the low frequency carbonyl component at 1702 cm^{-1} in Fig. 4.

The infrared data of Patel et al. on the solvation of esters and carbonates in various solvents indicate that this band can be assigned to C=O groups strongly hydrogen bonded to two water molecules [58]. The intensity of this subcomponent band is influenced by the incubation time at lower temperature and the formation kinetics is cation dependent. Fragata et al. have also shown this effect for PG:Mg^{2+} complexes [9,59].

The primary binding sites of the divalent cations, however, are exclusively the phosphodiester groups. Magnesium ions dehydrate the phosphate groups. Calcium and strontium ions change the conformation of the polar R–O–P–O–R′ head group. This change is also observed by comparing FTIR spectra of DMPG under physiological conditions and protonated DMPG (screening of charges). Tuchtenhagen [60] has explained this behavior by a variation of the usually found *gauche–gauche* conformation of this unit [47] to a *trans–trans* conformation. This can be induced by changes of the intermolecular interactions due to the reduction of electrostatic repulsion between head groups, e.g. induced by protonation or the presence of divalent cations. The antiplanar–antiplanar conformation of the R–O–P–O–R′ head group moiety in protonated DMPG and in the stable crystalline phases of DMPG:Ca^{2+} and DMPG:Sr^{2+} complexes is also supported by comparison with infrared spectra of the symmetric PO_2^- band in ox brain PS–Ca^{2+} and in DMPS–Ca^{2+} [41,51,55].

Finally, this investigation has demonstrated that the binding of divalent cations to negatively charged phospholipids like DMPG depends on the thermal history of the sample and that the rate of conversion from a metastable gel to a stable crystalline phase decreases in the order $Ca^{2+} \gg Mg^{2+} > Sr^{2+}$. This ranking is in accordance with the stability of the complexes, as estimated in our previous calorimetric study by the temperatures and enthalpies of the transition from the crystalline to the liquid crystalline state [31].

Although the lipid concentrations of 1–2 mM used in our calorimetric investigations were lower by a factor of 50–100 when compared to the concentrations applied in this FTIR study, the phase transition temperatures upon heating and cooling the DMPG:divalent cation complexes are approximately the same. For clarity, we have derived from our IR results a schematic picture for the conditions of conversion between stable and metastable phases in DMPG:divalent cation complexes (see Fig. 9).

The differences in the phase transition enthalpies between the stable crystalline/liquid crystalline states and the metastable gel/liquid crystalline states of these systems, as revealed in our previous paper [31] by DSC and ITC, are directly correlated with the results of this FTIR investigation, e.g. with changes of the hydrocarbon chain packing within the bilayers and with differences in the mobility of the lipid molecules. In addition, the small exo- and endothermic phase transitions, only observed in the second and third DSC heating scans of DMPG:Ca^{2+} between 35 and 55°C, can now unambiguously be assigned to a metastable crystalline/stable crystalline state phase transition, including primarily a reorientation of the lipid polar head groups. The conversion

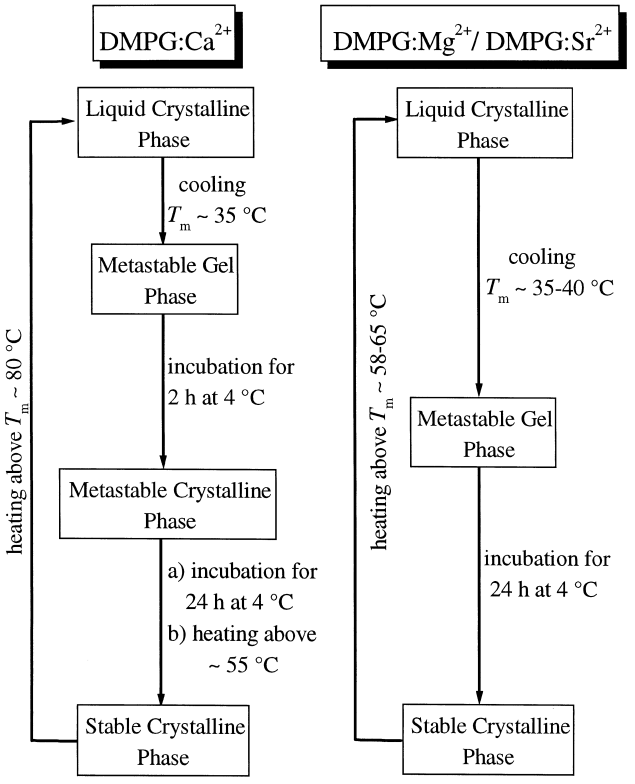

Fig. 9. Diagram of the observed phase states in DMPG:divalent cation complexes. The conditions for phase transitions are indicated along the arrows.

of DMPG:Ca^{2+} from a fluid state via a metastable gel to this metastable crystalline state was also suggested by the large reaction enthalpy of $\Delta H_R = 42$–46 kJ/mol in our ITC experiments, performed between 24 and 40°C [31]. The lower molar Ca^{2+}:lipid ratio of 1:1 in the IR experiments, compared to the ITC experiments (Ca^{2+}:lipid ratio >68:1), and the increased viscosity of the more highly concentrated samples prepared for the infrared spectroscopic investigations may be the reason for the time delay in the formation of the crystalline phases in this FTIR study.

In our ITC experiments we concluded from the difference molar heat capacity values ΔC_P that the binding of divalent cations (especially of Ca^{2+}) to DMPG in the gel phase induces dehydration of hydrophobic sites. Based on our IR spectra of the ester carbonyl stretching bands we infer that the interfacial region is still hydrated, but the mobility of the water molecules in the crystalline DMPG:divalent cation complexes is strongly reduced. For this reason the penetration of water molecules into the region of the hydrophobic methylene groups within the acyl chains may be minimized. A complete dehydration of the polar phosphate head group moiety is only observed in the crystalline complexes of DMPG:Mg^{2+}. However, in crystalline DMPG:Ca^{2+} and DMPG:Sr^{2+} complexes the head group orientation is different and therefore intra- or intermolecular hydrogen bonding of free glycerol OH groups to the phosphate groups may obscure the dehydration effect in the FTIR spectra of these systems.

In summary, this study has shown how different phases are induced by the binding of divalent cations to anionic lipids and it can be supposed that these interactions have large implications for different biological processes such as the stabilization of proteins in a lipid matrix.

References

[1] V. Koppaka, J.F. Wang, M. Banerjee, B.R. Lentz, Biochemistry 35 (1996) 7482–7491.
[2] S. Koppenol, F.H.C. Tsao, H. Yu, G. Zografi, Biochim. Biophys. Acta 1369 (1998) 221–232.
[3] P. Mustonen, J.Y.A. Lehtonen, P.K.J. Kinnunen, Biochemistry 37 (1998) 12051–12057.
[4] E.K. Nenonene, M. Methot, M. Fragata, Z. Naturforsch. C 53 (1998) 39–48.
[5] F.R. Poulain, S. Nir, S. Hawgood, Biochim. Biophys. Acta 1278 (1996) 169–175.
[6] S. Taneva, D.R. Voelker, K.M.W. Keough, Biochemistry 36 (1997) 8173–8179.
[7] D. Trommeshauser, H.J. Galla, Chem. Phys. Lipids 94 (1998) 81–96.
[8] D. Hoekstra, Biochemistry 21 (1982) 1055–1061.
[9] M. Fragata, E.K. Nenonene, V. Maire, I.S. Gabashvili, J. Mol. Struct. 405 (1997) 151–158.
[10] J.M. Boggs, G. Rangaraj, Biochemistry 22 (1983) 5424–5435.
[11] F. Borle, J. Seelig, Biochemistry 22 (1985) 5536–5544.
[12] B. de Kruijff, A.J. Verkleij, C.J.A. Leunissen-Dijvelt, C.J.A. van Echteld, J. Hille, H. Rijnbout, Biochim. Biophys. Acta 693 (1982) 1–12.
[13] A.J. Verkleij, B. de Kruyff, P.H. Ververgaert, J.F. Tocanne, L.L.M. van Deenen, Biochim. Biophys. Acta 339 (1974) 432–447.
[14] E.J. Findlay, P.G. Barton, Biochemistry 17 (1978) 2400–2405.
[15] B.D. Fleming, K.M.D. Keough, Chem. Phys. Lipids 49 (1988) 81–86.
[16] K. Harlos, H. Eibl, Biochemistry 19 (1980) 895–899.
[17] K. Jacobson, D. Papahadjopoulos, Biochemistry 14 (1975) 152–161.

[18] D. Papahadjopoulos, W.J. Vail, K. Jacobson, G. Poste, Biochim. Biophys. Acta 394 (1975) 483–491.
[19] D. Papahadjopoulos, J. Colloid Interface Sci. 58 (1977) 459–470.
[20] R.P. Rand, S. Segupta, Biochim. Biophys. Acta 255 (1972) 484–492.
[21] M. Roux, M. Bloom, Biophys. J. 60 (1991) 38–44.
[22] P.W.M. van Dijck, P.H.J.T. Ververgaert, A.J. Verkleij, L.L.M. van Deenen, J. de Gier, Biochim. Biophys. Acta 406 (1975) 465–478.
[23] P.W.M. van Dijck, B. de Kruijff, A.J. Verkleij, L.L.M. van Deenen, J. de Gier, Biochim. Biophys. Acta 512 (1978) 84–96.
[24] P.H.J.T. Ververgaert, B. de Kruyff, A.J. Verkleij, J.F. Tocanne, L.L.M. van Deenen, Chem. Phys. Lipids 14 (1975) 97–101.
[25] D.A. Wilkinson, D.A. Tirell, A.B. Turek, T.J. McIntosh, Biochim. Biophys. Acta 905 (1987) 447–453.
[26] D. Voelker, P. Smejtek, Biophys. J. 70 (1996) 818–830.
[27] L. Girault, A. Boudou, E.J. Dufourc, Biochim. Biophys. Acta 1414 (1998) 140–154.
[28] L. Lehrmann, J. Seelig, Biochim. Biophys. Acta 1189 (1994) 89–95.
[29] D. Papahadjopoulos, W.J. Vail, W.A. Pangborn, G. Poste, Biochim. Biophys. Acta 448 (1976) 265–283.
[30] G. Laroche, E.J. Dufourc, J. Dufourcq, M. Pézolet, Biochemistry 30 (1991) 3105–3114.
[31] P. Garidel, A. Blume, Langmuir 15 (1999) 5526–5534.
[32] R.G. Snyder, J. Mol. Spectrosc. 7 (1961) 116–144.
[33] R.G. Snyder, J. Chem. Phys. 47 (1967) 1316–1360.
[34] R.G. Snyder, S.L. Hsu, S. Krimm, Spectrochim. Acta A 34 (1978) 395–406.
[35] R.G. Snyder, H.L. Strauss, C.A. Elliger, J. Phys. Chem. 86 (1982) 5145–5150.
[36] H.L. Casal, H.H. Mantsch, Biochim. Biophys. Acta 779 (1984) 381–401.
[37] R. Mendelsohn, L. Senak, Adv. Spectrosc. 20 (1993) 339–380.
[38] L. Senak, M.A. Davies, R. Mendelsohn, J. Phys. Chem. 95 (1991) 2565–2571.
[39] W. Hübner, H.H. Mantsch, F. Paltauf, H. Hauser, Biochemistry 33 (1994) 320–326.
[40] H.L. Casal, A. Martin, H.H. Mantsch, F. Paltauf, H. Hauser, Biochemistry 26 (1987) 7395–7401.
[41] H.L. Casal, H.H. Mantsch, H. Hauser, Biochemistry 26 (1987) 4408–4416.
[42] R.N. Lewis, R.N. McElhaney, Biophys. J. 61 (1992) 63–77.
[43] Y.P. Zhang, R.N.A.H. Lewis, R.N. McElhaney, Biophys. J. 72 (1997) 779–793.
[44] A. Blume, W. Hubner, G. Messner, Biochemistry 27 (1988) 8239–8249.
[45] A. Blume, Colloid Interface Sci. 1 (1996) 64–77.
[46] W. Hübner, A. Blume, Chem. Phys. Lipids 96 (1998) 99–123.
[47] U.P. Fringeli, H.H. Günthard, Membr. Spectrosc. 31 (1981) 270–332.
[48] F.L. Hahn, R. Luckhaus, Z. Anal. Chem. 149 (1956) 172–177.
[49] R.G. Snyder, G.L. Liang, H.L. Strauss, R. Mendelsohn, Biophys. J. 71 (1996) 3186–3198.
[50] R.N.A.H. Lewis, R.N. McElhaney, W. Pohle, H.H. Mantsch, Biophys. J. 67 (1994) 2367–2375.
[51] R.A. Dluhy, D.G. Cameron, H.M. Mantsch, R. Mendelsohn, Biochemistry 22 (1983) 6318–6325.
[52] H.L. Casal, H.H. Mantsch, H. Hauser, Biochim. Biophys. Acta 982 (1989) 228–236.
[53] L. Senak, D. Moore, R. Mendelsohn, J. Phys. Chem. 96 (1992) 2749–2754.
[54] F.M. Goni, J.L. Arrondo, Faraday Discuss. Chem. Soc. 81 (1986) 117–126.
[55] H.L. Casal, H.H. Mantsch, F. Paltauf, H. Hauser, Biochim. Biophys. Acta 919 (1987) 275–286.
[56] H. Susi, Chem. Phys. Lipids 29 (1981) 359–368.
[57] P. Garidel, G. Förster, A. Blume, B.H. Kunst, G. Rapp, HASYLAB Annu. Rep. 2 (1998) 191–192.
[58] K.B. Patel, G. Eaton, M.C.R. Simons, J. Chem. Soc. Faraday Trans. 181 (1985) 2775–2786.
[59] M. Fragata, F. Bellemare, E.K. Nenonene, J. Phys. Chem. B 101 (1997) 1916–1921.
[60] J. Tuchtenhagen, Ph.D. Thesis, University of Kaiserslautern, 1994.